

# Cotunneling and nonequilibrium magnetization in magnetic molecular monolayers

Florian Elste<sup>1,\*</sup> and Carsten Timm<sup>2,†</sup>

<sup>1</sup>*Institut für Theoretische Physik, Freie Universität Berlin, Arnimallee 14, 14195 Berlin, Germany*

<sup>2</sup>*Department of Physics and Astronomy, University of Kansas, Lawrence, Kansas 66045, USA*

(Received 8 November 2006; revised manuscript received 27 March 2007; published 30 May 2007)

Transport and nonequilibrium magnetization in monolayers of magnetic molecules subject to a bias voltage are considered. We apply a master-equation approach going beyond the sequential-tunneling approximation to study the Coulomb-blockade regime. While the current is very small in this case, the magnetization shows changes of the order of the saturation magnetization for small variations of the bias voltage. Inelastic cotunneling processes manifest themselves as differential-conductance steps, which are accompanied by *much larger* changes in the magnetization. In addition, the magnetization in the Coulomb-blockade regime exhibits strong signatures of sequential tunneling processes *deexciting* molecular states populated by inelastic cotunneling. We also consider the case of a single molecule, finding that cotunneling processes lead to the occurrence of *magnetic sidebands* below the Coulomb-blockade threshold. In the context of molecular electronics, we study how additional spin relaxation suppresses the fine structure in transport and magnetization.

DOI: [10.1103/PhysRevB.75.195341](https://doi.org/10.1103/PhysRevB.75.195341)

PACS number(s): 73.63.-b, 85.65.+h, 73.23.Hk, 75.50.Xx

## I. INTRODUCTION

The idea of *molecular spintronics* consists of integrating the promising concepts of molecular electronics and spintronics.<sup>1-6</sup> A particularly interesting aspect of molecular electronics, besides the prospect of further miniaturization, is the possibility of using chemical synthesis for the fabrication of device components. This bottom-up process would start from relatively simple molecules and be massively parallel. In this context, spintronics is discussed in relation to magnetic memory<sup>7</sup> and quantum computation.<sup>8</sup> Both ideas rely on *magnetic* molecules.<sup>9</sup> Partly for this reason, electronic transport through magnetic molecules has recently received a lot of attention.<sup>10-23,26</sup>

Experimental research has focused on the fine structure of the Coulomb-blockade peaks<sup>10,11,16,17</sup> and on Kondo correlations in single-molecule transistors.<sup>10,11,27</sup> Furthermore, novel spin-blockade mechanisms and negative differential conductance have been observed.<sup>16,17</sup> These findings have also stimulated theoretical work, which mostly employs the sequential-tunneling approximation.<sup>13,15,18-21,23-25</sup> Like artificial quantum dots, a molecular junction is in the Coulomb-blockade regime at sufficiently small bias voltage, except at crossing points where two states with electron numbers differing by unity become degenerate. Due to the discreteness of molecular many-particle energies for weak coupling to the leads, there are typically no molecular transition energies in the window between the chemical potentials of the leads for small bias. In this regime, the very small tunneling current is not correctly described by the sequential-tunneling approximation. It is instead dominated by *cotunneling*, which appears in fourth order in the perturbation expansion in the tunneling amplitude. However, despite its experimental observation,<sup>17</sup> transport through magnetic molecules in this regime has been studied little.<sup>26</sup>

We study magnetic molecules under a bias voltage in the Coulomb-blockade regime. Our main result is that, while any features in the differential conductance are very small due to the suppression of the current, there are *large* changes in the average magnetic moments of the molecules with bias volt-

age and applied field. The measurement of magnetic moments of submonolayers of molecules has been demonstrated 20 years ago.<sup>28</sup> Even the detection of the spin of a single molecule may be feasible.<sup>29,30</sup> However, it is not clear how to perform such a measurement in a molecular-junction experiment. One recent experiment suggests that it is possible to employ carbon nanotube superconducting quantum interference devices for the detection of the switching of single magnetic moments.<sup>31</sup> Here, we mainly consider a *monolayer* of magnetic molecules between metallic electrodes, since the measurement of the magnetization of a thin film is expected to be easier than that of a single molecule. Various molecules form nearly perfect monolayers on metallic substrates.<sup>32</sup>

To find the current and the nonequilibrium magnetization, we use the master-equation formalism, treating the tunneling to the leads as a perturbation.<sup>13,18,19,33-35</sup> This approach describes the Coulomb and exchange interactions on the molecule *exactly* and works also far from equilibrium. In particular, it is not restricted to the linear-response regime of small bias voltage.

For memory applications, the control of spin relaxation is crucial. Since cotunneling and additional spin relaxation due to, e.g., dipolar and hyperfine interactions have similar selection rules for molecular transitions, consistency requires to include both. We find that spin relaxation is very effective in washing out the fine structure in the Coulomb-blockade regime, but may be used to advantage for the generation of spin-polarized currents.

## II. MODEL AND METHODS

For the most part, we consider a monolayer of magnetic molecules sandwiched between two metallic electrodes (see Fig. 1). We assume that magnetic interactions between the molecules are negligible and that all molecules have the same spatial orientation relative to the electrodes.<sup>32</sup> In this case, it is sufficient to consider the properties of a single molecule. Relaxation in the leads is assumed to be fast, so that their electron distributions can be described by equilib-

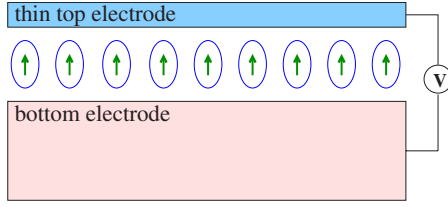


FIG. 1. (Color online) Sketch of the geometry. A monolayer of magnetic molecules is adsorbed on a metallic substrate, which serves as a bottom electrode. A thin metallic layer is used as a top electrode.

rium Fermi functions. In the simplest case, transport involves tunneling through only a single molecular level with on-site energy  $\epsilon_d$  and local Coulomb repulsion  $U$ . The full Hamiltonian of the system reads  $H = H_{\text{mol}} + H_{\text{leads}} + H_t$ , where<sup>18</sup>

$$H_{\text{mol}} = \epsilon_d n_d + \frac{U}{2} n_d (n_d - 1) - J \mathbf{s} \cdot \mathbf{S} - K_2 (S^z)^2 - B (s^z + S^z) \quad (1)$$

describes the molecular degrees of freedom,  $H_{\text{leads}} = \sum_{\alpha=L,R} \sum_{\mathbf{k}\sigma} \epsilon_{\alpha\mathbf{k}} a_{\alpha\mathbf{k}\sigma}^\dagger a_{\alpha\mathbf{k}\sigma}$  represents the two leads  $\alpha=L,R$  (left, right), and  $H_t = \sum_{\alpha=L,R} t_\alpha \sum_{\mathbf{k}\sigma} (a_{\alpha\mathbf{k}\sigma}^\dagger c_\sigma + c_\sigma^\dagger a_{\alpha\mathbf{k}\sigma})$  describes the tunneling. The tunneling amplitudes  $t_\alpha$  are chosen real. The operator  $c_\sigma^\dagger$  creates an electron with spin  $\sigma$  on the molecule.  $n_d \equiv c_\uparrow^\dagger c_\uparrow + c_\downarrow^\dagger c_\downarrow$  and  $\mathbf{s} \equiv \sum_{\sigma\sigma'} c_\sigma^\dagger \boldsymbol{\sigma}_{\sigma\sigma'} c_{\sigma'}/2$  are the corresponding number and spin operator, respectively. The parameter  $J$  denotes the exchange interaction between the electrons and a local spin  $\mathbf{S}$ , where  $\mathbf{S} \cdot \mathbf{S} = S(S+1)$ . We restrict ourselves to the case of easy-axis anisotropy,  $K_2 > 0$ . For simplicity, we consider identical  $g$  factors for  $\mathbf{s}$  and  $\mathbf{S}$ . An external magnetic field  $B$  is applied along the easy axis of the molecule, where a factor  $g\mu_B$  has been absorbed into  $B$ .  $a_{\alpha\mathbf{k}\sigma}^\dagger$  creates an electron in lead  $\alpha$  with spin  $\sigma$ , momentum  $\mathbf{k}$ , and energy  $\epsilon_{\alpha\mathbf{k}}$ .

The leading contribution to the transition rates between molecular many-particle states is of second order in  $H_t$ , corresponding to sequential tunneling. The transition rates can be obtained from Fermi's golden rule,<sup>35</sup>

$$\Gamma_\alpha^{nm'} = 2\pi \sum_\sigma t_\alpha^2 \nu_{\alpha\sigma} \{ f(\epsilon_m - \epsilon_n - \mu_\alpha) |C_{nm}^\sigma|^2 + [1 - f(\epsilon_n - \epsilon_m - \mu_\alpha)] |C_{mn}^\sigma|^2 \}. \quad (2)$$

Here, the eigenstates  $|n\rangle$  and  $|n'\rangle$  of  $H_{\text{mol}}$  denote the initial and final states of the molecule, respectively,  $\nu_{\alpha\sigma}$  is the density of states per unit cell of electrons with spin  $\sigma$  in lead  $\alpha$ ,  $f(\epsilon)$  is the Fermi function,  $\mu_\alpha$  is the chemical potential in lead  $\alpha$ , where  $\mu_L - \mu_R = -eV$ , and  $C_{nm}^\sigma \equiv \langle n | c_\sigma | n' \rangle$  is the matrix element of the electron annihilation operator between molecular many-particle states. The typical sequential-tunneling rate involving lead  $\alpha$  and electrons with spin  $\sigma$  is given by  $1/\tau_{\alpha\sigma} = 2\pi t_\alpha^2 \nu_{\alpha\sigma}$  ( $\hbar$  is set to unity).

To go beyond the leading order, the tunneling Hamiltonian is replaced by the  $T$  matrix,<sup>35</sup> which is self-consistently given by

$$T = H_t + H_t \frac{1}{E_i - H_0 + i\eta} T. \quad (3)$$

Here,  $E_i$  is the energy of the initial state  $|i\rangle|n\rangle$ , where  $|i\rangle$  refers to the equilibrium state of the left and right leads (at different chemical potentials) and  $|n\rangle$  is a molecular state. Furthermore,  $H_0 \equiv H_{\text{mol}} + H_{\text{leads}}$ , with the energy of the leads measured relative to equilibrium, and  $\eta$  is a positive infinitesimal, ensuring that the Green function in  $T$  is retarded. To fourth order, the transition rate from state  $|i\rangle|n\rangle$  to  $|f\rangle|n'\rangle$  with an electron tunneling from lead  $\alpha$  to lead  $\alpha'$  is given by

$$\Gamma_{\alpha\alpha'}^{n_i:n'_f} = 2\pi \left| \langle f | \langle n' | H_t \frac{1}{E_i - H_0 + i\eta} H_t | n \rangle | i \rangle \right|^2 \delta(E_f - E_i). \quad (4)$$

The energies of the initial state  $|n\rangle|i\rangle$  and final state  $|n'\rangle|f\rangle = |n'\rangle a_{\alpha'\mathbf{k}'\sigma'}^\dagger a_{\alpha\mathbf{k}\sigma} |i\rangle$  are denoted by  $E_i$  and  $E_f$ , respectively. We restrict ourselves to the case of infinite  $U$ ; i.e., double occupancy of the molecule is forbidden. Inserting  $H_t$  and summing over final lead states yield

$$\begin{aligned} \Gamma_{\alpha\alpha'}^{nn',00} &= 2\pi t_{\alpha'}^2 t_\alpha^2 \sum_{\sigma\sigma'} \nu_{\alpha\sigma} \nu_{\alpha'\sigma'} \\ &\times \int d\epsilon \left| \sum_{n''} \frac{C_{n'n''}^{\sigma'} C_{n''n'}^{\sigma*}}{\epsilon + \epsilon_n - \epsilon_{n''} + i\eta} \right|^2 \\ &\times f(\epsilon - \mu_\alpha) [1 - f(\epsilon + \epsilon_n - \epsilon_{n''} - \mu_{\alpha'})], \end{aligned} \quad (5)$$

$$\begin{aligned} \Gamma_{\alpha\alpha'}^{nn',11} &= 2\pi t_{\alpha'}^2 t_\alpha^2 \sum_{\sigma\sigma'} \nu_{\alpha\sigma} \nu_{\alpha'\sigma'} \\ &\times \int d\epsilon \left| \sum_{n''} \frac{C_{n'n''}^{\sigma'} C_{n''n'}^{\sigma*}}{-\epsilon + \epsilon_{n'} - \epsilon_{n''} + i\eta} \right|^2 \\ &\times f(\epsilon - \mu_\alpha) [1 - f(\epsilon + \epsilon_n - \epsilon_{n''} - \mu_{\alpha'})], \end{aligned} \quad (6)$$

where  $\Gamma_{\alpha\alpha'}^{nn',00}$  ( $\Gamma_{\alpha\alpha'}^{nn',11}$ ) denotes the cotunneling rate describing virtual transitions between two empty (singly occupied) molecular states. Here, we have assumed that the density of states in the leads is independent of energy. To the same order in  $H_t$ , one also obtains processes changing the electron number by  $\pm 2$ . For  $U \rightarrow \infty$ , these pair-tunneling processes<sup>36</sup> are suppressed. Note that Eqs. (5) and (6) contain both elastic and inelastic cotunneling.

Since the above expressions diverge due to second-order poles from the energy denominators, the cotunneling rates cannot be evaluated directly.<sup>37–40</sup> We apply a regularization scheme that follows Refs. 38–40 and is motivated by the observation that Eqs. (5) and (6) do not take into account the fact that the intermediate state obtains a finite width  $\Gamma$  due to tunneling. In our regime of weak tunneling, the width  $\Gamma$  is of second order in the tunneling amplitudes  $t_\alpha$ . This width is introduced into the energy denominators, replacing  $\eta$ . When the cotunneling rates are expanded in powers of  $\Gamma$ , it turns out that the leading term is of order  $1/\Gamma \propto 1/t_\alpha^2$ . This cancels two powers of the tunneling amplitude in Eqs. (5) and (6), so that the result is, in fact, a *sequential-tunneling* contribution.

Since we have already included the full sequential-tunneling rates, this new contribution should be dropped. We thus take the next order,  $\Gamma^0$ , for the cotunneling rates.

The *ad hoc* regularization of the cotunneling rate is not necessary in a description of cotunneling through wide quantum dots using nonequilibrium Green functions.<sup>41</sup> This approach avoids the divergences and also leads to a renormalization of transition energies at fourth order in the tunneling Hamiltonian. For a fully quantitative description of cotunneling through magnetic molecules, it would be desirable to employ this approach, which is, however, made complicated by the presence of the internal spin degree of freedom. On the other hand, the *T*-matrix approach used here is found to give qualitatively reasonable results in comparison with cotunneling experiments<sup>17</sup> and we expect it to catch the relevant physics for the system studied here.

The sequential and cotunneling rates appear in the rate equations for the probabilities of finding the molecule in state  $|n\rangle$  (we assume rapid dephasing<sup>13</sup>),

$$\frac{dP^n}{dt} = \sum_{am} (\Gamma_{\alpha}^{mn} P^m - \Gamma_{\alpha}^{nm} P^n) + \sum_{\alpha\alpha'm} (\Gamma_{\alpha\alpha'}^{mn} P^m - \Gamma_{\alpha\alpha'}^{nm} P^n), \quad (7)$$

where  $\Gamma_{\alpha\alpha'}^{mn} \equiv \Gamma_{\alpha\alpha'}^{mn,00} + \Gamma_{\alpha\alpha'}^{mn,11}$  and  $\Gamma_{\alpha\alpha'}^{mn,00}$  ( $\Gamma_{\alpha\alpha'}^{mn,11}$ ) is nonzero only if both  $|n\rangle$  and  $|m\rangle$  are empty (singly occupied). The current through the left lead is given by

$$I^L = -e \sum_{nm} (n_n - n_m) \Gamma_{L}^{mn} P^m - e \sum_{nm} (\Gamma_{LR}^{mn} - \Gamma_{RL}^{mn}) P^m. \quad (8)$$

The *steady-state* probabilities  $P^m$  of molecular states are obtained by solving Eq. (7) with the time derivatives set to zero. The average magnetization in the *z* direction per molecule is given by  $M = \sum_n m_n P^n$ , where  $m_n$  denotes the quantum number of the *z* component of the total spin  $\mathbf{s} + \mathbf{S}$  in state  $|n\rangle$ .

### III. RESULTS AND DISCUSSION

We start by discussing the results obtained for the differential conductance  $dI/dV$  at low bias voltages. If the system is in the Coulomb-blockade regime, sequential tunneling is thermally suppressed and transport is dominated by cotunneling. The magnitude of the current is then small. The conductance at zero bias voltage is finite [see Fig. 2(a)] due to *elastic* cotunneling. The cotunneling rates are proportional to the bias voltage if the molecular level is far from the chemical potentials, leading to ohmic behavior. The rounded steps in  $dI/dV$  correspond to the onset of additional *inelastic* cotunneling processes. Selection rules for the spin quantum number require  $\Delta m = 0, \pm 1$ . For the parameters chosen in Fig. 2, the ground state has electron number  $n=1$  and maximum spin  $m=5/2$ . Inelastic cotunneling processes corresponding to the two steps involve the two different final states with  $n=1$  and  $m=3/2$ , and virtual occupation of the state with  $n=0$  and  $m=2$ , as illustrated in Fig. 3. Further steps in  $dI/dV$  are not observed, since the corresponding inelastic cotunneling transitions have smaller energy differ-

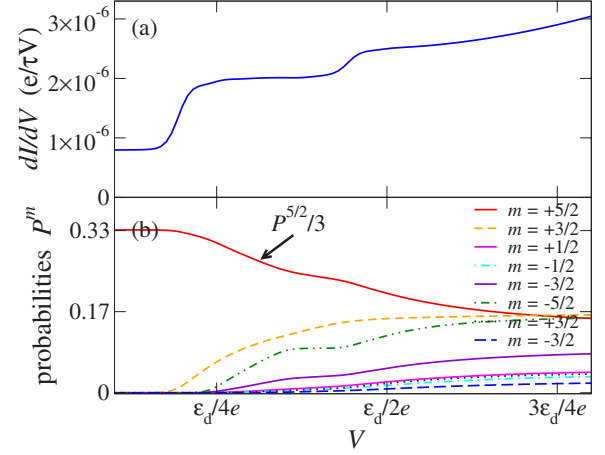


FIG. 2. (Color online) (a) Differential conductance  $dI/dV$  and (b) probabilities  $P^n$  of molecular many-particle states as functions of bias voltage  $V$ , for low bias voltages. The probability  $P^{5/2}$  of the ground state has been scaled by a factor of  $1/3$ . Here, we assume  $S=2$ ,  $J=K_2=5$  meV,  $\epsilon_d=10J$ ,  $B=2$  meV, and  $T=0.3$  meV (Ref. 42).

ences between initial and final states and are therefore activated immediately when the probability of the initial state becomes significant.

Cotunneling steps and sequential-tunneling peaks show fundamentally different dependences on the on-site energy  $\epsilon_d$ . For *single-molecule* junctions, it is possible to change  $\epsilon_d$  by applying a gate voltage, e.g., in molecular-junction experiments. For monolayers, one does not have this opportunity. We return to this point below. While the bias voltages at which sequential-tunneling peaks occur shift linearly with  $\epsilon_d$ , the positions of cotunneling steps remain unaffected. This follows directly from evaluating Eqs. (5) and (6) in the limit of large  $\epsilon_d$ .<sup>35</sup> For magnetic molecules, the position of the cotunneling steps shifts linearly as a function of the external magnetic field due to the Zeeman effect, as observed for  $\text{Mn}_{12}$ .<sup>17</sup>

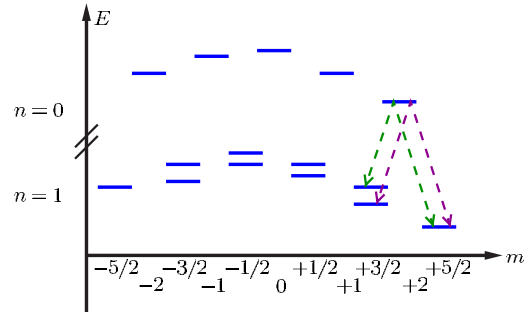


FIG. 3. (Color online) Level scheme showing the energies of molecular states as a function of magnetic quantum number  $m$  for electron numbers  $n=0, 1$  (Ref. 42). The dashed double arrows signify inelastic cotunneling between the ground state with  $m=5/2$  and the two states with  $m=3/2$ , involving virtual occupation of the state with  $n=0$  and  $m=2$ . While sequential tunneling requires a change of the electron number by  $\Delta n = \pm 1$  and of the magnetic quantum number by  $\Delta m = \pm 1/2$ , cotunneling processes obey the selection rules  $\Delta n = 0$  and  $\Delta m = 0, \pm 1$ .

While  $dI/dV$  represents the change of the *very small* current with bias voltage in the cotunneling regime, the change of the probabilities  $P^n$  of molecular states with bias voltage is of order unity, as shown in Fig. 2(b). The probability of the lowest-energy state with  $m=5/2$  decreases, whereas the probabilities of other states increase. Cotunneling enables transitions between molecular states with the same electron number, but with magnetic quantum numbers differing by  $\Delta m = \pm 1$ . These transitions are suppressed only as the inverse square of the energy difference between the initial state and the virtual state involved. In sequential tunneling, such transitions are also possible, requiring two consecutive steps, but are *exponentially* suppressed in the Coulomb-blockade regime. In the sequential-tunneling approximation, the molecule would thus remain in the lowest-energy state with essentially unit probability. This approximation is evidently invalid for determining the probabilities in this regime.

Interestingly, the strong effect of cotunneling on the probabilities also leads to observable effects of *sequential* tunneling on transport in the cotunneling regime.<sup>40,43</sup> While sequential tunneling starting from the lowest-energy state is exponentially suppressed, sequential tunneling from higher-energy states can be possible. With increasing bias voltage, these higher-energy states become increasingly populated due to cotunneling, as Fig. 2(b) shows. This leads to sidebands in  $dI/dV$  in the Coulomb-blockade regime that show the linear dependence on the gate voltage characteristic of sequential tunneling.<sup>40</sup> Strong electron-phonon coupling can enhance this effect, since it crucially affects the ratio of the rates for sequential and cotunneling processes.<sup>40</sup> In our case, these sidebands are very weak, since the current is controlled by the small cotunneling rates. However, we will see that the effect on the *probabilities*  $P^n$  of molecular states is significant.

Figure 4(a) shows the average magnetization per molecule as a function of bias voltage over a broad range including both the cotunneling and sequential-tunneling regimes. The magnetization is nonzero due to an external magnetic field. At zero bias, the molecule is in its ground state with  $m=5/2$ . The onset of inelastic cotunneling to the two states with  $m=3/2$  leads to a decrease in the magnetization in each case.

The bias-voltage dependence of the magnetization for voltages *above* the Coulomb-blockade threshold is accompanied by sizable steps in the current, as seen in Fig. 4(b). At each of these fine-structure steps, an additional inelastic sequential-tunneling transition becomes possible. The Coulomb-blockade threshold corresponds to the transition with initial state  $n=1$  and  $m=5/2$  and final state  $n=0$  and  $m=2$ . Therefore, the onset of sequential tunneling is accompanied by a *decrease* in the magnetization. At large bias the magnetization drops to zero, since all states are occupied with equal probability.

Remarkably, pronounced steplike features are also present *below* the Coulomb-blockade threshold in Fig. 4(a), where the current is due to cotunneling and thus very small [cf. Figs. 4(b) and 4(c)]. This can be understood from the bias-voltage dependence of the relevant probabilities  $P^n$  in Fig. 4(d). As an example, consider the step marked by an arrow in Fig. 4(a). The physics leading to the drastic change of the

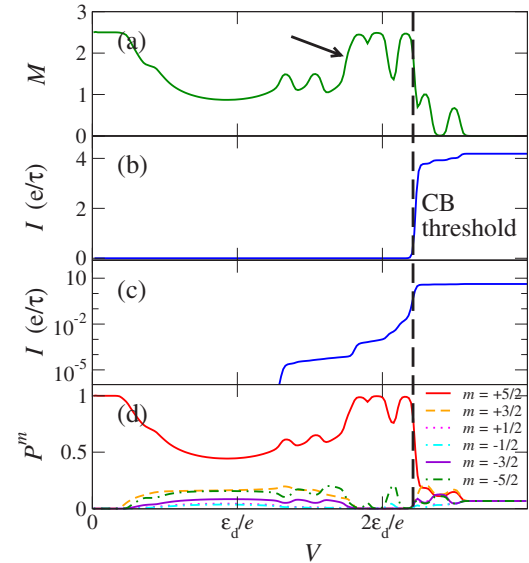


FIG. 4. (Color online) (a) Magnetization  $M$ , (b) linear plot of the current  $I$ , (c) logarithmic plot of the sequential-tunneling current, and (d) probabilities  $P^n$  of various molecular many-particle states as functions of bias voltage  $V$ . The parameters are chosen as in Fig. 2.

probabilities is illustrated in Fig. 5: The sequential-tunneling processes with  $m=-3/2 \rightarrow -2$ ,  $m=-1/2 \rightarrow -1$ ,  $m=3/2 \rightarrow 2$ , and  $m=1/2 \rightarrow 1$ , starting at the higher-energy level of each pair (thin arrows in Fig. 5), are already energetically possible at lower bias voltages, causing the partial depopulation of the initial states. However, the probabilities of these states are nonzero mainly due to cotunneling processes (dashed arrows in Fig. 5). Below the step marked in Fig. 4(a), the half-integer spin states with positive and negative  $m$  are *not connected* by sequential-tunneling processes. As soon as the transition with  $m=-1/2 \rightarrow 0$  (bold arrow in Fig. 5) becomes possible, the states with positive and negative  $m$  are connected and fast sequential-tunneling processes depopulate all states except for the ground state, which has  $m=5/2$ . Con-

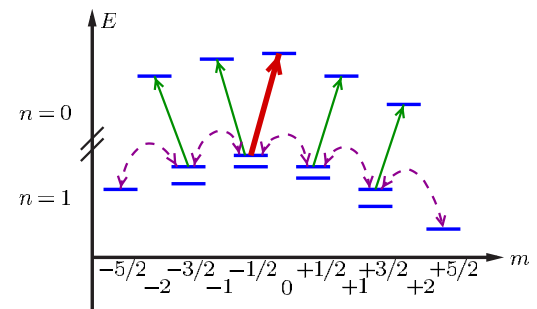


FIG. 5. (Color online) Level scheme illustrating the interplay between sequential tunneling (solid arrows) and cotunneling (dashed arrows) in magnetic molecules (Ref. 42). Even below the Coulomb-blockade threshold, sequential-tunneling processes starting from higher-energy states populated by cotunneling may cause the depopulation of these states and drastically affect the average magnetization. At the step denoted by an arrow in Fig. 4(a), the excitation of the transition with  $m=-1/2 \rightarrow 0$  (heavy solid arrow) gives rise to a redistribution of the probabilities  $P^n$ . Note that exothermal transitions with  $\Delta m = \pm 1/2$  are always possible.

sequently, the average magnetization again approaches its maximum value. Similarly, one can attribute each step to a particular molecular transition. As Fig. 4(c) shows, the onsets of *some* of these sequential-tunneling processes can also be seen in the sequential-tunneling current, which is, however, small in the cotunneling regime.

The above discussion shows that quantities that depend strongly on the probabilities of molecular states, such as the magnetization, are much more sensitive to changes of the bias voltage in the Coulomb-blockade regime than the conductivity. This suggests using the *magnetization-voltage* characteristics, i.e., the magnetization as a function of bias voltage, instead of the current-voltage characteristics to extract the excitation spectrum of magnetic molecules. In order to distinguish magnetic transitions from, e.g., vibrational excitations, one should analyze their dependence on the magnetic field. Furthermore, for a monolayer there is no gate voltage that can serve as an independent parameter. The magnetic field can assume this role.

Figure 6(a) shows a density plot of the magnetization as a function of bias voltage and magnetic field. The magnetization is an odd function of the field. The transition energies shift linearly with the field,  $\Delta E = \Delta m B$ , if the initial and final states have magnetic quantum numbers differing by  $\Delta m$ .

Complementary to conventional differential-conductance plots, the density plots in Fig. 6 can serve as fingerprints of the internal degrees of freedom of the molecules. The Zeeman splitting of the molecular levels due to the external magnetic field gives rise to triangular plateaus with a tip at  $B=0$ . These plateaus are bounded by two sequential-tunneling transitions. In each case, these two transitions differ in the sign of the magnetic quantum number  $m$  of both initial and final molecular states. For the chosen parameters, the plateaus can be attributed to the following transitions from empty to singly occupied states, starting at low bias voltage (cf. Fig. 5):  $|m|=3/2 \rightarrow 2$ ,  $|m|=1/2 \rightarrow 1$ ,  $|m|=1/2 \rightarrow 0$ ,  $|m|=3/2 \rightarrow 2$ ,  $|m|=3/2 \rightarrow 1$ ,  $|m|=1/2 \rightarrow 1$ ,  $|m|=5/2 \rightarrow 2$  (this is the first transition starting from the ground state and thus represents the Coulomb-blockade threshold),  $|m|=1/2 \rightarrow 0$ , and  $|m|=3/2 \rightarrow 1$ . Several transitions appear twice because there are two states with magnetic quantum numbers  $\pm 3/2$  and  $\pm 1/2$ , respectively. For a local spin  $S=2$ , there exist nine transitions obeying the selection rule  $\Delta m = \pm 1/2$ , as can be seen from Fig. 5, in accordance with the nine plateaus shown in Fig. 6(a). Note again that the signal is similar on both sides of the Coulomb-blockade threshold.

The origin of the plateaus is schematically illustrated in Fig. 6(e) for the transition  $|m|=1/2 \rightarrow 0$ . In the absence of an external Zeeman field, the excitation energies for both transitions is equal. However, the excitation energies differ by the Zeeman energy as soon as a magnetic field is switched on. This leads to the occurrence of a finite bias-voltage window, where the excitation of one of the two transitions is energetically possible whereas the other one is not. Inside this window, only the spin-down state is depopulated by sequential tunneling, leading to a large positive magnetization.

So far, we have restricted ourselves to the situation where the relaxation of the local molecular spin is dominated by electron tunneling, i.e., the spin is *conserved* between tunneling events. However, there are other processes that also con-

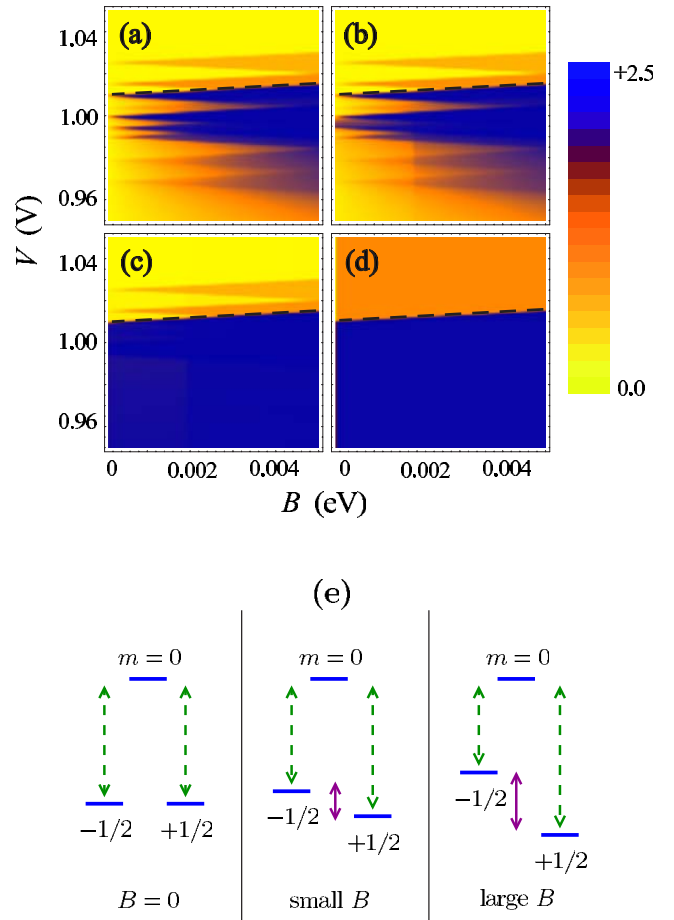


FIG. 6. (Color online) Magnetization  $M$  as a function of bias voltage  $V$  and magnetic field  $B$  for different spin-relaxation times: (a)  $t_{\text{rel}} = \infty$ , (b)  $t_{\text{rel}} = 10^6 \tau$ , (c)  $t_{\text{rel}} = 10^2 \tau$ , and (d)  $t_{\text{rel}} = 0$ . Here,  $\tau = (2\pi t_{\alpha}^2 \nu_{\alpha})^{-1}$  denotes the typical electronic tunneling time, assuming symmetric coupling to the leads. All other parameters are chosen as above. The dashed lines denote the Coulomb-blockade threshold. (e) Level schemes illustrating the origin of the magnetization plateaus.

tribute to spin relaxation: (i) Magnetic molecules containing transition-metal ions, such as  $\text{Mn}_{12}$  clusters, show strong spin-orbit interaction, which leads to spin relaxation. (ii) Hyperfine interactions with nuclear magnetic moments in the molecule can also lead to spin relaxation. However, in molecules one has the chance to essentially remove this mechanism by choosing isotopes with vanishing nuclear spins. (iii) Dipolar interactions with spins of other molecules in the monolayer or with impurity spins in the electrodes contribute to spin relaxation. (iv) Small nonuniaxial magnetic anisotropies lead to tunneling between the eigenstates of  $H_{\text{mol}}$ . This mechanism has recently been discussed in the context of transport through magnetic molecules.<sup>14–16</sup>

All these processes change the magnetic quantum number while keeping the electron number constant ( $\Delta n = 0$ ). The dominant transitions are the ones with  $\Delta m = \pm 1$ . These are the same selection rules as for cotunneling, indicating that one should include additional spin relaxation for consistency when studying cotunneling.

The effect of spin relaxation on the electronic transport is included in the formalism by a phenomenological rate  $\propto 1/t_{\text{rel}}$ , which forces the system to approach the equilibrium distribution on the time scale  $t_{\text{rel}}$ . We include additional transition rates between states  $|n\rangle$  and  $|m\rangle$  with  $\Delta n=0$  and  $\Delta m = \pm 1$ ,  $\Gamma_{nm}^{\text{rel}} = \exp[(\epsilon_n - \epsilon_m)/kT]/t_{\text{rel}}$  for  $\epsilon_n < \epsilon_m$  and  $\Gamma_{nm}^{\text{rel}} = 1/t_{\text{rel}}$  otherwise. The additional rates obey detailed balance, ensuring relaxation towards equilibrium in the absence of tunneling.

Effects of spin relaxation on the bias-voltage dependence of the magnetization are illustrated in Figs. 6(a)–6(c) and 6(d). For small  $t_{\text{rel}}$  (fast relaxation), the number of transitions appearing as steps in the magnetization-voltage characteristics is reduced, since spin relaxation depopulates higher-energy states that serve as initial states for these transitions.

The magnetization plateaus start to occur when the relaxation time  $t_{\text{rel}}$  becomes significantly larger than the typical sequential-tunneling time  $\tau = (2\pi t_{\alpha}^2 \nu_{\alpha})^{-1}$ . (The sequential-tunneling time enters because the relevant process is the depopulation of states by sequential tunneling.) Then the time spent by the electron on the molecule is smaller than the spin relaxation time so that magnetic excitations survive between tunneling events.

So far, we have considered a monolayer of magnetic molecules, mostly because the measurement of the magnetization is easier for larger numbers of molecules. As mentioned previously, even the detection of a *single* molecular spin might be feasible.<sup>29,30</sup> Using a single molecule allows one to introduce a gate electrode in order to tune the molecular energy levels by shifting  $\epsilon_d$  [see Eq. (1)]. In the following, we briefly discuss results obtained for varying gate voltage. To increase the magnetization signal while retaining the gate electrode, one might consider a one-dimensional array of magnetic molecules or even a large number of such arrays aligned in parallel.

The plot of the magnetization and the differential conductance as functions of bias voltage and on-site energy  $\epsilon_d$  presented in Figs. 7(a) and 7(c) shows two striking features. First, the magnetization shows steps indicating the onset of inelastic cotunneling, which are almost independent of  $\epsilon_d$ . The corresponding steps in  $dI/dV$  are very small in absolute units [see Fig. 2(a)]. Second, the magnetization shows strong additional magnetic sidebands in the Coulomb-blockade regime. These sidebands are the consequence of sequential-tunneling transitions depopulating molecular states that are populated by cotunneling, as discussed above. In  $dI/dV$ , the corresponding features are completely hidden by the low-bias tail of the large peak at the Coulomb-blockade threshold (not shown). The observation of these sidebands in the Coulomb-blockade regime requires long spin-relaxation times compared to the typical tunneling time. For fast spin relaxation, fine-structure peaks are only present in the sequential-tunneling regime [see Fig. 7(b)], since sequential tunneling is still faster than spin relaxation, even though cotunneling is slower. As shown in Fig. 7(d), the absence of such sidebands is accompanied by suppressed fine-structure peaks in the sequential-tunneling regime.

Finally, we note that sufficiently fast spin relaxation leads to *spin-polarized* stationary currents in the presence of a magnetic field. If the spin of the magnetic molecule relaxes

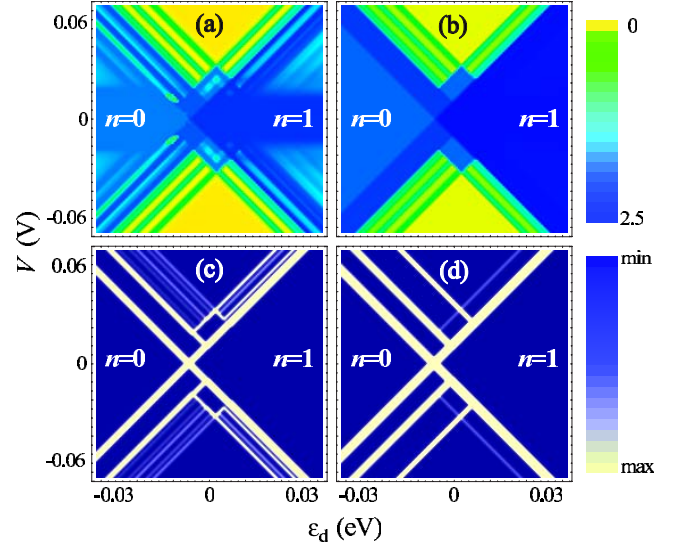


FIG. 7. (Color online) [(a) and (b)] Magnetization  $M$  and [(c) and (d)] differential conductance of a single magnetic molecule as a function of  $V$  and  $\epsilon_d$  for [(a) and (c)] slow spin relaxation,  $t_{\text{rel}} = 10^{10}\tau$ , and [(b) and (d)] fast spin relaxation,  $t_{\text{rel}} = \tau$ . We assume  $S=2$ ,  $J=K_2=5$  meV,  $T=0.1$  meV, and  $B=2$  meV.

fast compared to the typical tunneling rate, which is essentially determined by the current, the system is always in its ground state. Due to the Zeeman effect, the ground state has maximum magnetic quantum number;  $m=5/2$  for our example. Thus only spin-down electrons can tunnel onto the molecule, resulting in a spin-polarized current. Note that this argument is not restricted to low-order perturbation theory in  $H_t$ . As shown in Fig. 8, the degree of spin polarization is basically determined by the ratio of the spin-relaxation rate and the typical electronic tunneling rate.

#### IV. CONCLUSIONS

In summary, we have studied the interplay of electronic transport through magnetic molecules and their nonequilibrium magnetic moment beyond the sequential-tunneling ap-

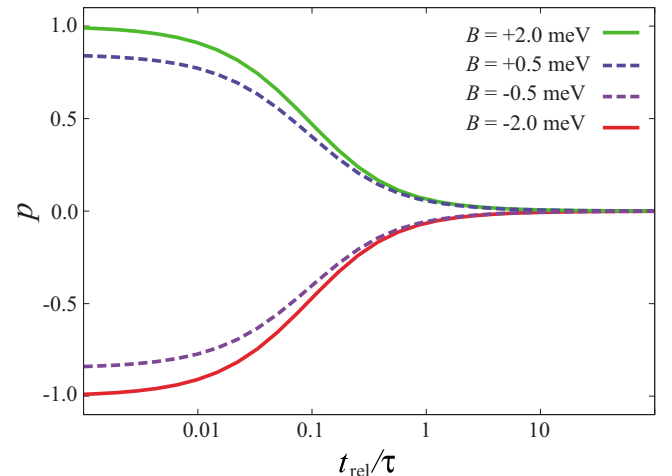


FIG. 8. (Color online) Polarization of the current,  $p \equiv (I^{L\uparrow} - I^{L\downarrow})/(I^{L\uparrow} + I^{L\downarrow})$ , as a function of spin-relaxation time  $t_{\text{rel}}$  in units of the typical tunneling time  $\tau$ .

proximation. We have focused mostly on monolayers, which should give a better chance of measuring the magnetization than single molecules would.

While the excitation of inelastic tunneling processes in the Coulomb-blockade regime leads only to a very small absolute change in the current, the change of the probabilities of finding the molecule in various many-particle states is significant. This manifests itself in a strong bias-voltage dependence of the magnetization. The magnetization of a molecular monolayer can be switched by an amount of the order of the saturation magnetization by a small change of bias voltage, and without causing the flow of a large current.

We find steps in the differential conductance due to inelastic cotunneling, which have been observed in experiments on  $\text{Mn}_{12}$ .<sup>17</sup> These steps are accompanied by much larger changes in the magnetization. Another interesting effect is the appearance of additional sidebands in the Coulomb-blockade regime that can be ascribed to *deexcitations* by sequential tunneling of states populated by cotunneling. These sidebands are very prominent in the magnetization. We suggest that the magnetization, or any measurable quantity that strongly differs between molecular states, can

be employed to study molecular transitions that are, from the point of view of transport, hidden in the Coulomb-blockade regime.

For spintronics applications, the ability to control the persistence of the stored information is crucial. In this context, we have considered effects of additional spin relaxation in the same formalism. Our results show that for sufficiently fast spin relaxation, the peaks in the differential conductance and the steps in the magnetization are washed out, as expected. At the same time, the degree of polarization of the steady-state current contains information about the ratio of the spin-relaxation rate and the typical electronic tunneling rate. Fast spin relaxation, while, in general, undesirable, can lead to a highly polarized current in the presence of a magnetic field.

### ACKNOWLEDGMENTS

We would like to thank J. Koch and F. von Oppen for valuable discussions. Support by the Deutsche Forschungsgemeinschaft through Sonderforschungsbereich 658 is gratefully acknowledged.

\*Electronic address: felste@physik.fu-berlin.de

†Electronic address: ctimm@ku.edu

- <sup>1</sup>S. A. Wolf, D. D. Awschalom, R. A. Buhrman, J. M. Daughton, S. von Molnár, M. L. Roukes, A. Y. Chtchelkanova, and D. M. Treger, *Science* **294**, 1488 (2001).
- <sup>2</sup>I. Žutić, J. Fabian, and S. Das Sarma, *Rev. Mod. Phys.* **76**, 323 (2004).
- <sup>3</sup>S. Sanvito and A. R. Rocha, *J. Comput. Theor. Nanosci.* **3**, 624 (2006).
- <sup>4</sup>E. G. Emberly and G. Kirczenow, *Chem. Phys.* **281**, 311 (2002); *Phys. Rev. Lett.* **91**, 188301 (2003).
- <sup>5</sup>A. Nitzan and M. A. Ratner, *Science* **300**, 1384 (2003).
- <sup>6</sup>Y. Xue and M. A. Ratner, *Phys. Rev. B* **68**, 115406 (2003); **68**, 115407 (2003); *Nanotechnology: Science and Computation*, edited by J. Chen, N. Jonoska, and G. Rozenberg (Springer-Verlag, Berlin, 2006).
- <sup>7</sup>C. Joachim, J. K. Gimzewski, and A. Aviram, *Nature (London)* **408**, 541 (2000).
- <sup>8</sup>W. Harneit, *Phys. Rev. A* **65**, 032322 (2002).
- <sup>9</sup>S. J. Blundell and F. L. Pratt, *J. Phys.: Condens. Matter* **16**, R771 (2004).
- <sup>10</sup>J. Park, A. N. Pasupathy, J. I. Goldsmith, C. Chang, Y. Yaish, J. R. Petta, M. Rinkoski, J. P. Sethna, H. D. Abruña, P. L. McEuen, and D. C. Ralph, *Nature (London)* **417**, 722 (2002).
- <sup>11</sup>W. Liang, M. P. Shores, M. Bockrath, J. R. Long, and H. Park, *Nature (London)* **417**, 725 (2002).
- <sup>12</sup>J. Paaske and K. Flensberg, *Phys. Rev. Lett.* **94**, 176801 (2005).
- <sup>13</sup>F. Elste and C. Timm, *Phys. Rev. B* **71**, 155403 (2005).
- <sup>14</sup>C. Romeike, M. R. Wegewijs, W. Hofstetter, and H. Schoeller, *Phys. Rev. Lett.* **96**, 196601 (2006).
- <sup>15</sup>C. Romeike, M. R. Wegewijs, and H. Schoeller, *Phys. Rev. Lett.* **96**, 196805 (2006).
- <sup>16</sup>H. B. Heersche, Z. de Groot, J. A. Folk, H. S. J. van der Zant, C. Romeike, M. R. Wegewijs, L. Zoppi, D. Barreca, E. Tondello, and A. Cornia, *Phys. Rev. Lett.* **96**, 206801 (2006).
- <sup>17</sup>M.-H. Jo, J. E. Grose, K. Baheti, M. M. Deshmukh, J. J. Sokol, E. M. Rumberger, D. N. Hendrickson, J. R. Long, H. Park, and D. C. Ralph, *Nano Lett.* **6**, 2014 (2006).
- <sup>18</sup>C. Timm and F. Elste, *Phys. Rev. B* **73**, 235304 (2006).
- <sup>19</sup>F. Elste and C. Timm, *Phys. Rev. B* **73**, 235305 (2006).
- <sup>20</sup>M. N. Leuenberger and E. R. Mucciolo, *Phys. Rev. Lett.* **97**, 126601 (2006).
- <sup>21</sup>A. Donarini, M. Grifoni, and K. Richter, *Phys. Rev. Lett.* **97**, 166801 (2006).
- <sup>22</sup>C. Romeike, M. R. Wegewijs, W. Hofstetter, and H. Schoeller, *Phys. Rev. Lett.* **97**, 206601 (2006).
- <sup>23</sup>M. Misiorny and J. Barnas, arXiv:cond-mat/0610556 (unpublished).
- <sup>24</sup>V. N. Golovach and D. Loss, *Phys. Rev. B* **69**, 245327 (2004).
- <sup>25</sup>G.-H. Kim and T.-S. Kim, *Phys. Rev. Lett.* **92**, 137203 (2004).
- <sup>26</sup>G. Gonzalez and M. N. Leuenberger, arXiv:cond-mat/0610653 (unpublished).
- <sup>27</sup>J. J. Parks, A. R. Champagne, G. R. Hutchison, S. Flores-Torres, H. D. Abruña, and D. C. Ralph, arXiv:cond-mat/0610555 (unpublished).
- <sup>28</sup>M. Zomack and K. Baberschke, *Surf. Sci.* **178**, 618 (1986); *Phys. Rev. B* **36**, R5756 (1987).
- <sup>29</sup>C. Durkan and M. E. Welland, *Appl. Phys. Lett.* **80**, 458 (2002).
- <sup>30</sup>D. Rugar, R. Budakian, H. J. Mamin, and B. W. Chui, *Nature (London)* **430**, 329 (2004).
- <sup>31</sup>J.-P. Cleuziou, W. Wernsdorfer, V. Bouchiat, T. Ondarçuhu, and M. Monthieux, *Nature Nanotechnology (London)* **1**, 53 (2006).
- <sup>32</sup>C. Zhou, M. R. Deshpande, M. A. Reed, L. Jones II, and J. M. Tour, *Appl. Phys. Lett.* **71**, 611 (1997).
- <sup>33</sup>A. Mitra, I. Aleiner, and A. J. Millis, *Phys. Rev. B* **69**, 245302 (2004).

- <sup>34</sup>K. Blum, *Density Matrix Theory and Applications* (Plenum, New York, 1981).
- <sup>35</sup>H. Bruus and K. Flensberg, *Many-body Quantum Theory in Condensed Matter Physics* (Oxford University Press, Oxford, 2004).
- <sup>36</sup>J. Koch, M. E. Raikh, and F. von Oppen, Phys. Rev. Lett. **96**, 056803 (2006).
- <sup>37</sup>D. V. Averin, Physica B **194–196**, 979 (1994).
- <sup>38</sup>M. Turek and K. A. Matveev, Phys. Rev. B **65**, 115332 (2002).
- <sup>39</sup>J. Koch, F. von Oppen, Y. Oreg, and E. Sela, Phys. Rev. B **70**, 195107 (2004).
- <sup>40</sup>J. Koch, F. von Oppen, and A. V. Andreev, Phys. Rev. B **74**, 205438 (2006).
- <sup>41</sup>J. König, H. Schoeller, and G. Schön, Phys. Rev. Lett. **78**, 4482 (1997); Phys. Rev. B **58**, 7882 (1998).
- <sup>42</sup>Since we wish to exhibit the general physical effects expected in (co-)tunneling through monolayers, the parameters are chosen in such a way that these effects are most clearly seen. The parameters do not correspond to a specific molecule. Note that a large exchange interaction,  $JS^2 \gg K_2S$ , which is appropriate for some molecules, does not change this physics—in Figs. 3 and 5 it would just shift the  $n=1$  spin quartet to high energies, possibly above the  $n=0$  quintet, which would not interfere with the mechanism of large magnetization changes.
- <sup>43</sup>B. LeRoy, S. Lemay, J. Kong, and C. Dekker, Nature (London) **432**, 371 (2004).